Diyala Journal for Pure Science



# Charge Density Distributions and Nuclear Radii of Some Sd-Shell Nuclei

**Ahmed N. Abdullah**

Department of Physics - College of Science - University of Baghdad - Baghdad - Iraq

Ahmednajim@scbaghdad.edu.iq

**Received: 24 March 2020** **Accepted: 1 September 2020**

DOI: https://dx.doi.org/10.24237/djps.16.04.530A

## Abstract

The ground state charge and matter density distributions, the corresponding root mean square (rms) radii and the elastic electron scattering form factors for some sd-shell nuclei (such as $^{23}$Na, $^{25}$Mg, $^{27}$Al and $^{29}$Si nuclei) are studied by the radial wave functions of the harmonic oscillator (HO) and Woods-Saxon (WS) potentials. The calculated results are discussed and compared with the experimental data. It is found that the calculated results of charge and matter density distributions are in very good agreement with the experimental data.

**Keywords**: Woods-Saxon potential, Harmonic oscillator potential, Charge density distributions, Elastic electron scattering, Nuclear radii.

Diyala Journal for Pure Science

# Charge Density Distributions and Nuclear Radii of Some Sd-Shell Nuclei

Ahmed N. Abdullah

# توزيعات الكثافة الشحنية وانصاف الاقطار النووية لبعض نوى القشرة النووية sd

أحمد نجم عبدالله

قسم الفيزياء - كلية العلوم - جامعة بغداد – بغداد - العراق

## الخلاصة

تم دراسة توزيعات الكثافة الشحنية والمادية مع انصاف الاقطار المرافقة لها وعوامل التشكل للاستطارة الالكترونية المرنة لبعض النوى الواقعة ضمن القشرة النووية sd باستخدام الدوال الموجية القطرية لجهدي المتذبذب التوافقي وودز-ساكسون. تم مقارنة النتائج المحسوبة مع القيم العملية وتم الحصول على توافق جيد بين توزيعات الكثافة الشحنية والمادية مع القيم العملية.

**الكلمات المفتاحية:** جهد وودز-ساكسون، جهد المتذبذب التوافقي، توزيعات الكثافة الشحنية ، الاستطارة الالكترونية المرنة، انصاف الاقطار النووية.

## Introduction

In the nuclear structure the most important quantities are the form factors and charge density distributions (CDD) which are well studied experimentally for a wide range of nuclei. Moreover, the distribution of density is an important object for theoretical and experimental investigations because in nuclear theory it plays the role of a fundamental variable [1]. One of the powerful tools to investigate the CDD for stable nuclei is electron–nucleus scattering [2,3]. We can obtain information about the charges distribution within the nucleus by measuring the elastic cross sections.

The most important nuclear potential used to describe the interaction between the single nucleon and whole nuclei is the Woods–Saxon potential. This potential is widely used in nuclear reactions, nuclear structure, particle physics and nuclear scattering. The Woods–Saxon basis used as better choice than harmonic oscillator basis in both non-relativistic and relativistic theories of nuclear mean-field shell model to study the nuclear structure, nuclear decay and electromagnetic transitions [4].

Abdullah [5] has calculated the charge density distributions in the ground state, elastic electron scattering form factors and the corresponding rms radii for some 1p-shell nuclei with $Z = N$ (such as $^{6}$Li, $^{10}$B, $^{12}$C and $^{14}$N nuclei) using the single particle radial wave functions of harmonic oscillator (HO) and Woods-Saxon (WS) potentials. The calculated results were discussed and compared with the experimental data. Abdullah [6] has used the Skyrme parameters namely; SGII, SKxtb, SKxs15, SKxs20, SKO and SKxs25 within the Skyrme–Hartree–Fock (SHF) method to investigate the proton, charge and matter densities, the corresponding rms radii and neutron skin thickness for some *sd*-shell nuclei with *Z*=*N* (such as; $^{20}$Ne, $^{24}$Mg, $^{28}$Si and $^{32}$S). The results obtained were compared with the experimental results. The calculated results showed a good agreement with experimental data.

In this work, we study the ground state charge and matter density distributions, the corresponding root mean square (rms) radii and the elastic electron scattering form factors for some sd-shell nuclei such as $^{23}$Na, $^{25}$Mg, $^{27}$Al and $^{29}$Si nuclei using the single particle radial wave functions of the harmonic oscillator (HO) and Woods-Saxon (WS) potentials and compared the calculated results with the available experimental results.

## Theory

The matter density distributions are given as [7]:

$$\rho_m(r) = \rho_p(r) + \rho_n(r), \quad (1)$$

Where $\rho_p(r)$ and $\rho_n(r)$ are the proton and neutron density distributions, respectively which can be written as [8]:

$$\rho_p(r) = \frac{1}{4\pi}\sum_{n\ell j} X_p^{n\ell j}\left|R_{n\ell j}\right|^2 \quad (2)$$

$$\rho_n(r) = \frac{1}{4\pi}\sum_{n\ell j} X_n^{n\ell j}\left|R_{n\ell j}\right|^2 \quad (3)$$

where $X_{p(n)}^{n\ell j}$ is the number of protons or neutrons in the $n\ell j$ -subshell.

The normalization conditions for the ground state densities given in eqs. (1-3) are:

$$g = 4\pi \int_0^\infty \rho_g(r)\ r^2 dr, \tag{4}$$

where $\rho_g(r)$ corresponds to the one of the densities $[\rho_p(r),\ \rho_n(r),\ \rho_m(r)]$ and $g$ corresponds to the number of nucleons in each case.

In this study, two methods are utilized for calculating the ground state densities of nuclei under study namely HO and WS.

In the HO method, the proton, neutron and matter density distributions are described by the HO radial wave function that given by [9]:

$$R_{n\ell}(r) = \frac{1}{(2\ell+1)!!}\left[\frac{2^{\ell-n+3}(2n+2\ell-1)!!}{\sqrt{\pi}b^3(n-1)!}\right]\left(\frac{r}{b}\right)^{\ell} e^{-r^2/2b^2} \sum_{k=0}^{n-1}(-1)^k \frac{(n-1)!\,2^k(2\ell+1)!!}{(n-k-1)!\,k!\,(2\ell+2k+1)!!}\left(\frac{r}{b}\right)^{2k} \tag{5}$$

Where $b = \sqrt{\hbar/\,M_p\omega}$ is the HO size parameter (which is the length parameter for the HO well), $M_p$ is the mass of the proton and $\omega$ is the angular frequency.

In the WS method, the proton, neutron and matter density distributions are described by the WS radial wave function which are taken from the solution to radial part of the Schrodinger equation using WS potential which given as [10]:

$$\frac{d^2R_{n\ell j}(r)}{dr^2} + \frac{2\mu}{\hbar^2}\left[\varepsilon_{n\ell j} - V(r) - \frac{\hbar^2}{2\mu}\frac{\ell(\ell+1)}{r^2}\right]R_{n\ell j}(r) = 0 \tag{6}$$

Where $R_{n\ell j}(r)$ the radial eigenfunction of WS potential, $\varepsilon_{n\ell j}$ is the single particle binding energy, $n, \ell$ and $j$ are the principle, orbital angular and total quantum numbers and $\mu$ is the reduced mass of the core and single nucleon $\mu = m(A-1/A)$, A is the nuclear mass number and m is the nucleon mass.

The local potential [V(r)] can be written as [11]:

$$V(r) = V_0(r) + V_{so}(r)\boldsymbol{L}.\boldsymbol{S} + V_c(r), \quad (7)$$

Where $V_0(r)$ is the central potential takes the form of WS potential [11]:

$$V_0(r) = -\frac{V_0}{1+e^{(r-R_0)/a_0}} \quad (8)$$

$V_0$ is depth of central potential.

$V_{so}(r)$ is the spin-orbit potential expressed as [11]:

$$V_{so}(r) = V_{so}\frac{1}{r}\left[\frac{d}{dr}\frac{1}{(1+e^{(r-R_{so})/a_{so}})}\right] \quad (9)$$

$V_{so}$ is depth of spin-orbit potential.

and $V_c(r)$ is the Coulomb potential (for protons only) generated by a homogeneous charged sphere of radius $R_c$ [12]:

$$V_c(r) = \begin{cases} \frac{Ze^2}{r} & \text{for} \quad r > R_c \\ \frac{Ze^2}{R_c}\left[\frac{3}{2} - \frac{r^2}{2R_c^2}\right] & \text{for} \quad r \le R_c \end{cases} \quad (10)$$

and $V_c(r) = 0$ for neutrons.

The radii $R_0$,$R_{so}$ and $R_c$ are usually expressed as [12]:

$$R_i = r_i A^{1/3} \quad , i = 0, so \; or \; c \quad (11)$$

Where $A$ is the nuclear mass number

From the proton density $\rho_p(r)$ and the intrinsic charge distribution $f_p$ of one proton, we can obtain the charge distribution of the nucleus with the following folding relation [12]:

$$\rho_{ch}(r) = \int \rho_p(r) f_p(r' - r)\, dr' \quad (12)$$

Where $f_p$ takes the Gaussian form as follows [12]:

$$f_p(r) = \frac{1}{(\sqrt{\pi}a_p)^3} e^{(-r^2/a_p^2)} \quad (13)$$

The charge and matter rms radii can be written as [13]:

$$r_g = \langle r_g^2 \rangle^{1/2} = \left[ \frac{\int r^2 \rho_g(r) dr}{\int \rho_g(r) dr} \right]^{1/2} \qquad g = m, ch \tag{14}$$

The elastic form factor in the plane wave Born approximation (PWBA) is given by [12]:

$$F(q) = \frac{4\pi}{Z} \int_0^\infty \rho_{ch}(r) j_0(qr) r^2 dr \tag{15}$$

Where $j_0(qr)$ is the spherical Bessel function of order zero and $q$ is the momentum transfer from the incident electron to the target nucleus.

## Results and discussion

The ground state charge and matter density distributions and the corresponding rms radii for some sd-shell nuclei (such as $^{23}$Na, $^{25}$Mg, $^{27}$Al and $^{29}$Si nuclei) are studied by the radial wave functions of the HO and WS potentials. The elastic charge form factors of these nuclei are studied through combining the charge density distributions with the plane-wave Born approximation (PWBA).

The WS parameters are chosen to reproduce the single particle binding energies of Ref. [14] because of the absence of available experimental single particle binding energies for selected nuclei. Table 1 displays the WS parameters used in the present study.

**Table 1:** The WS parameters employed in the present study

| Nuclei | $V_0$ (MeV) | $V_{so}$ (MeV) | $a_0 = a_{so}$ (fm) | $r_0 = r_{so}$ (fm) | $r_c$ (fm) |
|---|---|---|---|---|---|
| $^{23}$Na | 59.294 | 6.0 | 0.819 | 1.312 | 1.371 |
| $^{25}$Mg | 55.838 | 6.0 | 0.765 | 1.278 | 1.361 |
| $^{27}$Al | 56.673 | 6.0 | 0.759 | 1.292 | 1.353 |
| $^{29}$Si | 58.527 | 6.0 | 0.771 | 1.281 | 1.346 |

The charge and matter rms radii are calculated by the HO and WS potentials for $^{23}$Na, $^{25}$Mg, $^{27}$Al and $^{29}$Si nuclei and tabulated in Table-2 along with the experimental results [15-18]. It is clear from this table that the obtained results are in a good agreement with experimental results

within quoted error. The calculated results of the single-particle energies (ε) for the selected nuclei along with those of Ref. [14] are displayed in table 3.

**Table 2:** Comparison between the experimental and calculated results of charge and matter rms radii measured in fermi units

| Nuclei | $\langle r_{ch}^2 \rangle^{1/2}$ | | $\langle r_{ch}^2 \rangle_{exp}^{1/2}$ | $\langle r_m^2 \rangle^{1/2}$ | | $\langle r_m^2 \rangle_{exp}^{1/2}$ |
|---|---|---|---|---|---|---|
| | HO | WS | [15,16] | HO | WS | [17,18] |
| $^{23}$Na | 2.993 | 3.026 | 2.993±0.002 | 2.937 | 2.946 | 2.93±0.03 |
| $^{25}$Mg | 3.036 | 3.102 | 3.11±0.05 | 2.974 | 3.013 | 2.96±0.25 |
| $^{27}$Al | 3.105 | 3.149 | 3.061±0.003 | 3.040 | 3.056 | 3.093±0.009 |
| $^{29}$Si | 3.142 | 3.173 | 3.13±0.05 | 3.068 | 3.078 | ---- |

**Table 3:** The calculated single particle binding energies for $^{23}$Na, $^{25}$Mg, $^{27}$Al and $^{29}$Si nuclei

| *Nuclei* | $n\ell j$ | *proton* | | *neutron* | |
|---|---|---|---|---|---|
| | | $\varepsilon_{cal}$ (MeV) | $\varepsilon_l$ (MeV) [14] | $\varepsilon_{cal}$ (MeV) | ε (MeV) [14] |
| $^{23}$Na | $1s_{1/2}$ | 35.382 | 35.382 | 40.337 | 40.337 |
| | $1p_{3/2}$ | 23.241 | 23.241 | 27.830 | 27.830 |
| | $1p_{1/2}$ | 20.750 | 20.750 | 25.345 | 25.345 |
| | $1d_{5/2}$ | 10.969 | 10.969 | 15.167 | 15.167 |
| $^{25}$Mg | $1s_{1/2}$ | 32.732 | 32.732 | 38.081 | 38.081 |
| | $1p_{3/2}$ | 20.970 | 20.970 | 25.937 | 25.937 |
| | $1p_{1/2}$ | 18.455 | 18.455 | 23.432 | 23.432 |
| | $1d_{5/2}$ | 9.001 | 9.001 | 13.556 | 13.556 |
| $^{27}$Al | $1s_{1/2}$ | 34.185 | 34.185 | 39.910 | 39.910 |
| | $1p_{3/2}$ | 22.789 | 22.789 | 28.123 | 28.123 |
| | $1p_{1/2}$ | 20.458 | 20.458 | 25.809 | 25.809 |
| | $1d_{5/2}$ | 11.019 | 11.019 | 15.945 | 15.945 |
| $^{29}$Si | $1s_{1/2}$ | 35.728 | 35.728 | 41.840 | 41.840 |
| | $1p_{3/2}$ | 24.363 | 24.363 | 30.076 | 30.076 |
| | $1p_{1/2}$ | 22.117 | 22.117 | 27.849 | 27.849 |
| | $1d_{5/2}$ | 12.571 | 12.571 | 17.872 | 17.872 |
| | $1d_{5/2}$ | ---- | ---- | 13.795 | 13.795 |

Figures 1(a) - 1(d) show the calculated CDD's for $^{23}$Na,$^{25}$Mg, $^{27}$Al and $^{29}$Si nuclei, respectively obtained by the HO potential (red curve) and WS potential (blue curve) along with the experimental data (filled circle symbols) [15,19]. It is evident from these figures that both of

the red and blue curves are in very good agreement with the experimental data except a slight deviation appearing in the calculated results at the region of small *r*.

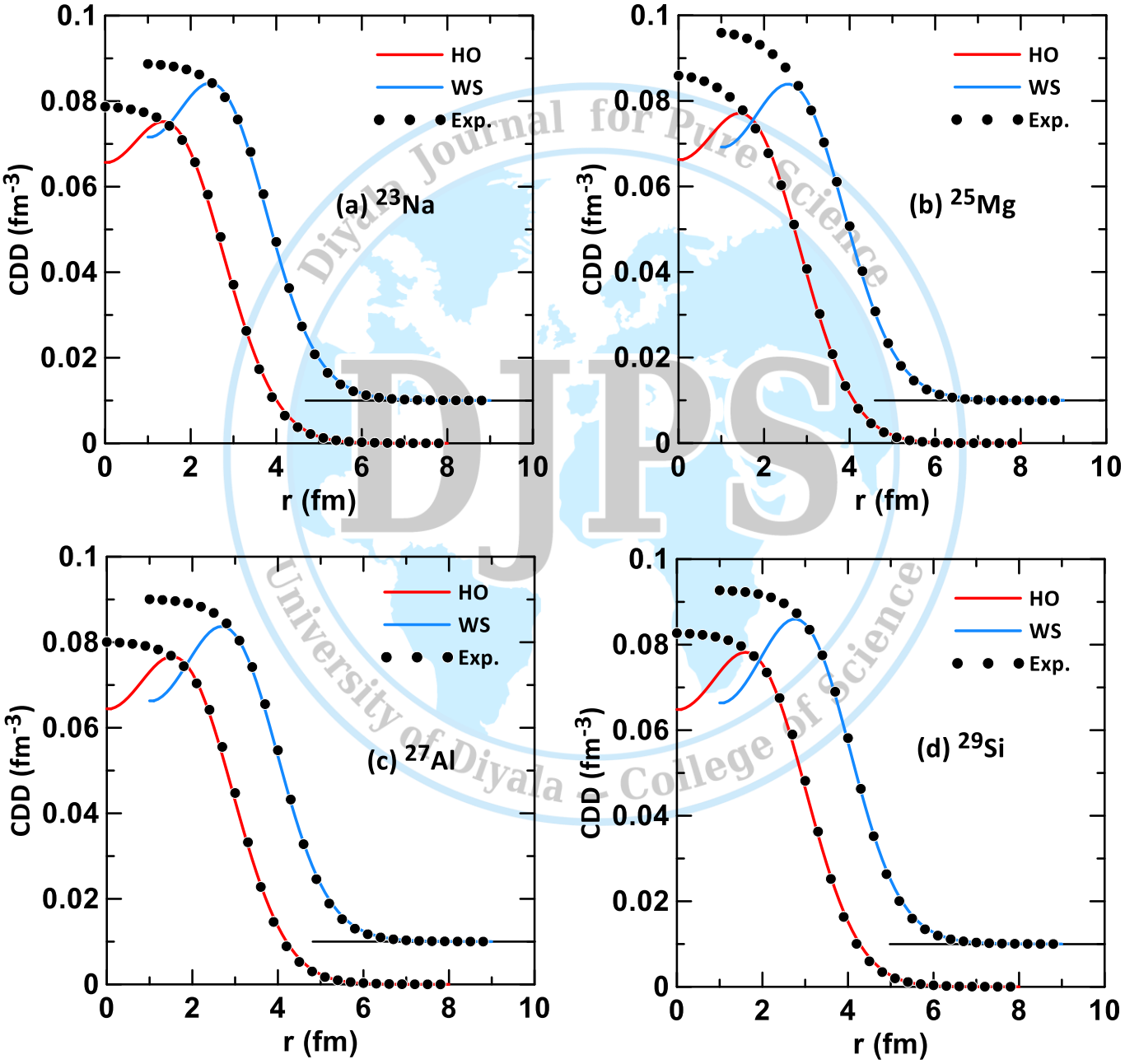


**Figure 1:** The calculated CDD's for $^{23}$Na, $^{25}$Mg, $^{27}$Al and $^{29}$Si nuclei. The blue curve and data have been progressively offset by 1 fm and 0.01 in the charge density.

Fig. 2 illustrates the calculated matter density distributions (MDD's) for $^{23}$Na [Fig. 2(a)], $^{25}$Mg [Fig. 2(b)], $^{27}$Al [Fig. 2(c)] and $^{29}$Si [Fig. 2(d)] nuclei obtained by HO potential (red curves) and WS potential (blue curves). For comparison the experimental matter densities (filled circle symbols) of these nuclei [15,19] are also shown in this figure. It is clearly shown from this figure that the calculated matter density distributions for these nuclei underestimate the experimental results at the region of small *r* whereas beyond this region the calculated results agree very well with the experimental data.

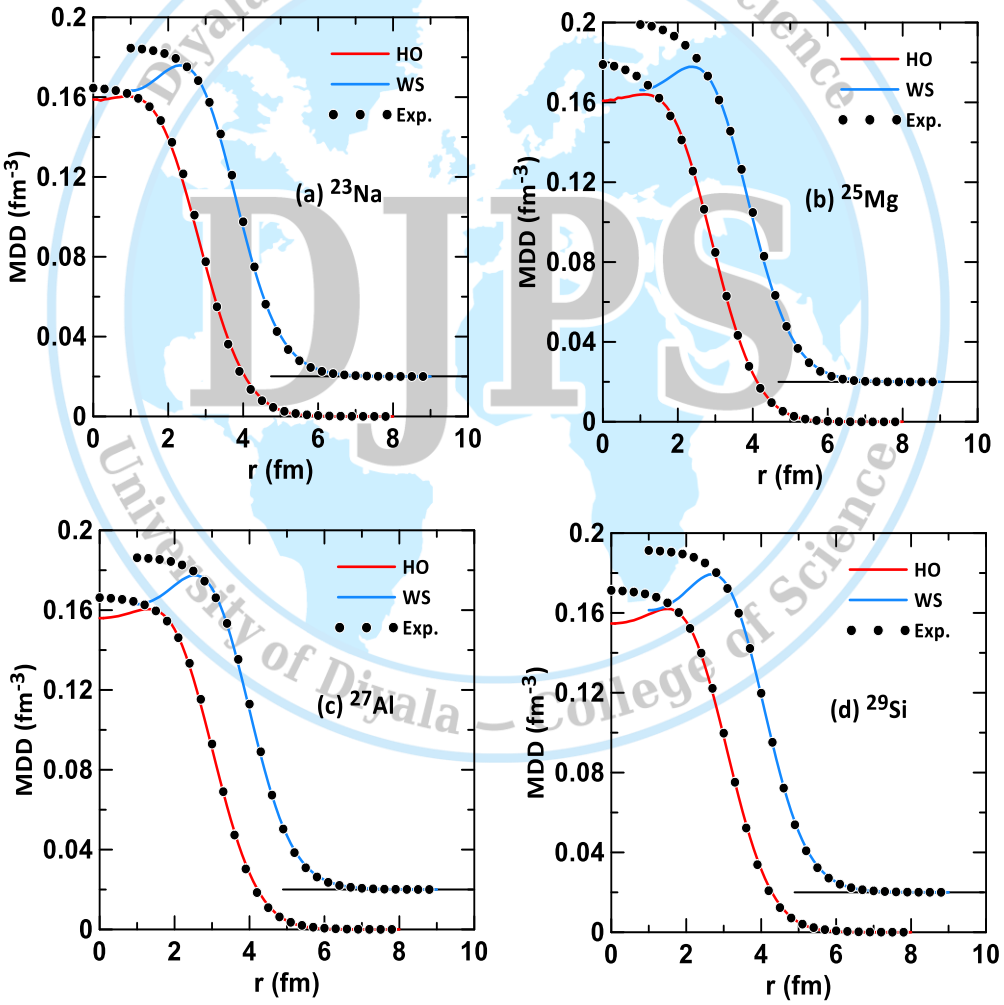


**Figure 2:** The calculated and experimental MDD's for $^{23}$Na, $^{25}$Mg, $^{27}$Al and $^{29}$Si nuclei. The blue curve and data have been progressively offset by 1 fm and 0.02 in the matter density

Fig. 3 presents the elastic charge form factors obtained by HO (red curve) and WS (dashed-blue curve) potentials for $^{23}$Na [Fig.3(a)], $^{25}$Mg [Fig.3(b)], $^{27}$Al [Fig.3(c)] and $^{29}$Si [Fig.3(d)] nuclei. The experimental data of $^{23}$Na [15], $^{25}$Mg [20], $^{27}$Al [21] and $^{29}$Si [19] are denoted by the open circle symbols. From this figure we can see that both red and dashed-blue curves are in very good accordance with the open circle symbols. Moreover, both the red and dashed-blue curves succeed in reproducing the first diffraction minimum of the experimental data.

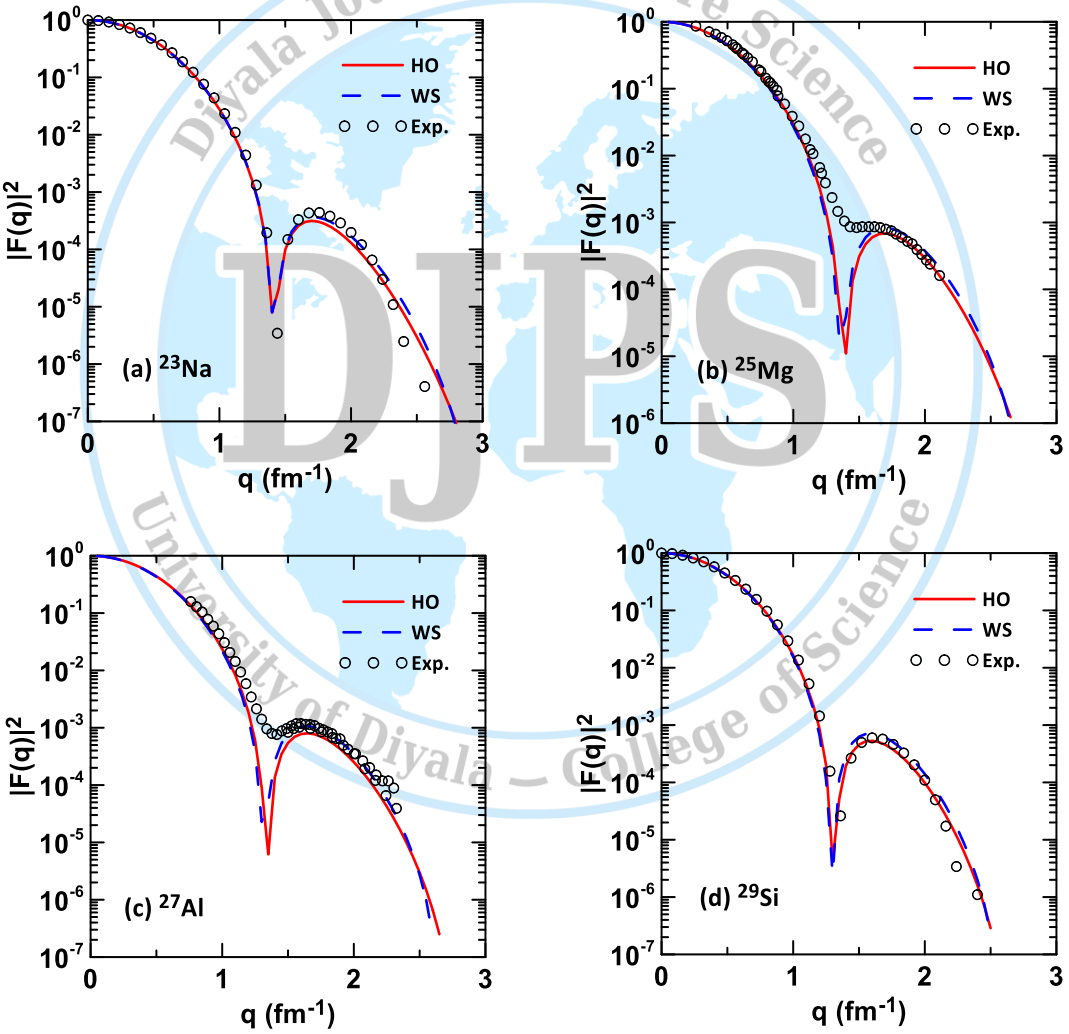


**Figure 3:** The elastic charge form factors for $^{23}$Na, $^{25}$Mg, $^{27}$Al and $^{29}$Si nuclei

## Conclusions

The ground state charge and matter density distributions, the corresponding rms radii and the elastic electron scattering form factors for some sd-shell nuclei (such as $^{23}$Na, $^{25}$Mg, $^{27}$Al and $^{29}$Si nuclei) are studied by the radial wave functions of the HO and WS potentials. The calculated results are discussed and compared with the experimental data. It is found that the calculated results of charge and matter density distributions are in very good agreement with the experimental data except a slight deviation appearing in the calculated results at the region of small *r*. The calculated charge and matter rms radii for the investigated nuclei are in a good agreement with the experimental data. The calculated results of the elastic charge form factors obtained in both of the HO and WS potentials show a good agreement with experimental data.

## References

1. A. N. Antonov, P. E. Hodgson, I. Zh. Petkov, Nucleon Momentum and Density Distributions in Nuclei, (Clarendon Press, Oxford, 1988).
2. T. W. Donnelly, I. Sick, Reviews of Modern Physics, 56 ,461(1984)
3. A. H. Wapstra, G. Audi, R. Hoekstra, Atomic masses from (mainly) experimental data, *Atomic Data and Nuclear Data Tables*, 39 ,281(1988)
4. M.R. Pahlavani , S.A. Alavi, *commun. Theor. Phys.* ,58 ,739(2012)
5. A. N. Abdullah, *International Journal of Chem.Tech. Research*, 10 (6) ,956(2017)
6. A.N. Abdullah, *Iraqi Journal of Physics*, 15 ,21(2017)
7. A.N. Antonov, D.N. Kadrev, M.K. Gaidarov, E.M. de Guerra, P. Sarriguren, J.M. Udias, V.K. Lukyanov, E.V. Zemlyanaya, G.Z. Krumova, *Physical Review C*,72 ,044307(2005)
8. B. A. Brown, S. E. Massent, P. E. Hodgson, *J. Phys. G: Nucl. Phys.* , 5 ,1655(1979)
9. P. J. Brussard, P. W. M. Glaudemans, Shell-Model Application in Nuclear spectroscopy, (North-Holland, Amesterdam ,1977)
10. A. N. Abdullah, *Int. J. Mod. Phys. E*, 26 ,1750048(2017)
11. A. N. Abdullah, *Journal of Al-Nahrain University* ,20 ,42(2017)
12. A. N. Abdullah, *Int. J. Mod. Phys. E*, 29 ,2050015(2020)

**13.** A. N. Abdullah, *Pramana. J. Phys.*, 89 ,43(2017)

**14.** B. A. Brown, W. D. M. Rae, *Nucl. Data Sheets*, 120 ,115(2014)

**15.** H. de Vries, C.W. de Jager, C. de Vries, *At. Data Nucl. Data Tables*, 36 ,495(1987)

**16.** I. Angeli, K. P. Marinova, *Atomic Data and Nuclear Data Tables* ,99 ,69(2013)

**17.** S. Ahmad, A. A. Usmani, Z. A. Khan, *Phys. Rev. C*, 96 ,064602(2017)

**18.** 18- F. G. Wei *et al.*, *Chin. Phys. C*, 33, 1(2009)

**19.** 19- G. Fricke, C. Bernhardt, K. Heilig, L.A. Schaller, L. Schellenberg, E.B. Shera, C.W. Dejager, *Atomic Data and Nuclear Data Tables* ,60 ,177(1995)

**20.** H. Euteneuer, H. Rothhaas, O. Schwentker, J.R. Moreira, C.W. De Jager, L. Lapikas, H. De Vries, J. Flanz, K. Itoh, G.A. Peterson, D.V. Webb, *Physical Review C* ,16 ,1703(1977)

**21.** G. C. Li, M. R. Yearian , I. Sick, *Phys. Rev. C* ,9 ,1861(1974).